Supporting Information

Identification of kinases and interactors of p53 using kinase-catalyzed crosslinking and immunoprecipitation (K-CLIP)

Satish Garre, Aparni K. Gamage, Todd R. Faner, Pavithra Dedigama-Arachchige, and Mary Kay H. Pflum

Department of Chemistry, Wayne State University, 5101 Cass Avenue, Detroit, MI 48202

Table of Contents **Page**

I. Experimental Procedures

Materials

Cell culture grade dimethylsulfoxide (DMSO) was purchased from ATCC. The disodium salt of Adenosine 5'-triphosphate (ATP.2Na), glycerol, sodium hydroxide (NaOH), potassium chloride (KCl), magnesium chloride ($MgCl_2$), sodium chloride (NaCl), sodium dodecyl sulfate (SDS), and glacial acetic acid were purchased from Fisher. Ammonium bicarbonate, tris(2-carboxyethyl) phosphine HCl (TCEP), iodoacetamide, and proteomics grade trypsin were bought from Sigma. Triton X-100 was purchased from Fluka. Coomassie Brilliant Blue was obtained from NuSep. Trifluoroacetic acid (TFA) and Immobilion-P PVDF membrane were purchased from Millipore. SyproRuby stain was obtained from Invitrogen. Eagle's minimum essential medium (EMEM) (30-2003) and RKO cell culture sample (CRL-2577) were purchased from ATCC. Acrylamide/Bis acrylamide solution (40%, 37.5:1) was purchased from Bio-Rad. Proteomics grade formic acid was purchased from Proteochem. Protein A/G-PLUS agarose beads (SC-2003), p53 (rabbit) polyclonal antibody (SC-6243), and p53 (mouse) monoclonal antibody (SC-55476) were purchased from Santa Cruz Biotechnology Inc. DNA-PK antibody (4602P) and rabbit IgG HRP-linked secondary antibody (7074) were purchased from Cell Signaling Technology. Fetal bovine serum (FBS), antibiotic-antimycotic (100X), TrypLE™ Express (1X) with Phenol Red and Alexa Fluor® 647 Goat Anti-Rabbit IgG (H+L) (A-21244) were purchased from Life Technologies. Goat anti-mouse IgG (H+L) (HRP) (ab97040) secondary antibody was purchased from Abcam. Goat anti-mouse HiLyte Fluor™ 647-labeled secondary antibody was purchased from Anaspec. FNK antibody (GTX111495) was obtained from Genetex Inc. (±) Nutlin-3 was purchased from Cayman Chemicals.

Instrumentation

A SPD131 DDA ThermoSavant speedvac was used to evaporate solvents *in vacuo*. SDS-PAGE apparatus was purchased from BioRad (Protean III) and a mini-gel setup was used. Western blotting was carried out using the mini-transblot electrophoretic transfer Cell apparatus from Bio-Rad. Western blot and SDS-PAGE gel images were visualized using a Typhoon 9210 scanner (Amersham Biosciences). A model 3UV-38 UV lamp (UVP, Inc.) was used for crosslinking experiments.

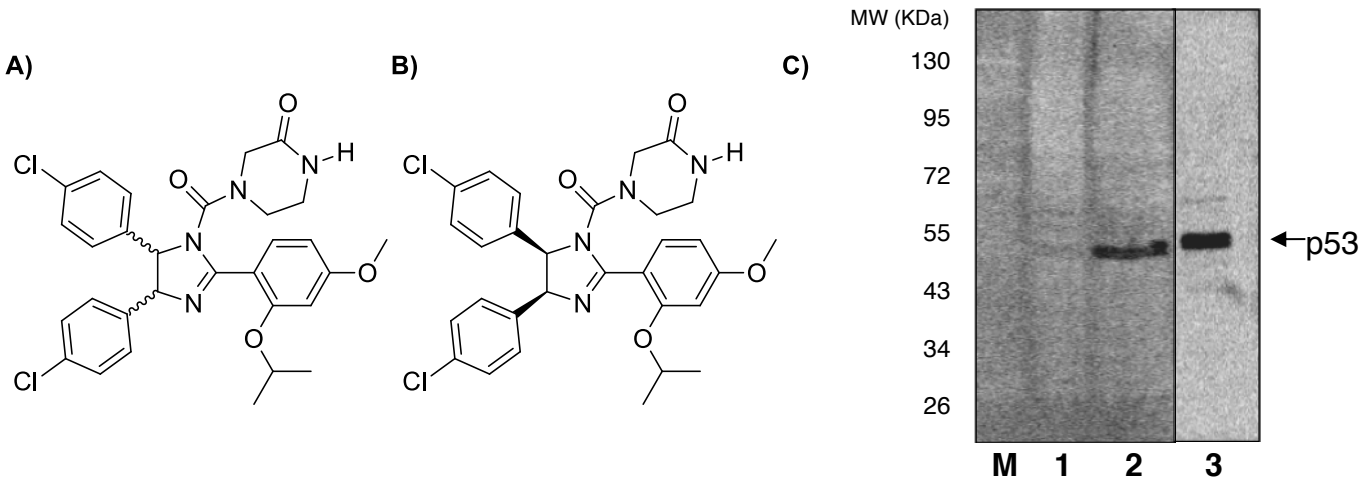

Figure S1. Treatment of RKO cells with (±)-Nutlin. (A) Chemical structure of (±)-Nutlin-3 (B) Chemical structure of (-)-Nutlin-3, the active enantiomer (C) SDS-PAGE separation and anti-p53 western blot analysis of lysates obtained after RKO cells were treated with (±)-Nutlin-3. The contents of each lane are: molecular weight marker (M), DMSO treated control cell lysates (lane 1), (±)-Nutlin-3 (10 μM) treated cell lysates (lane 2), and (±)-Nutlin-3 (20 μM) treated cell lysates (lane 3). The expected 53 kDa p53 protein band is indicated with an arrow.

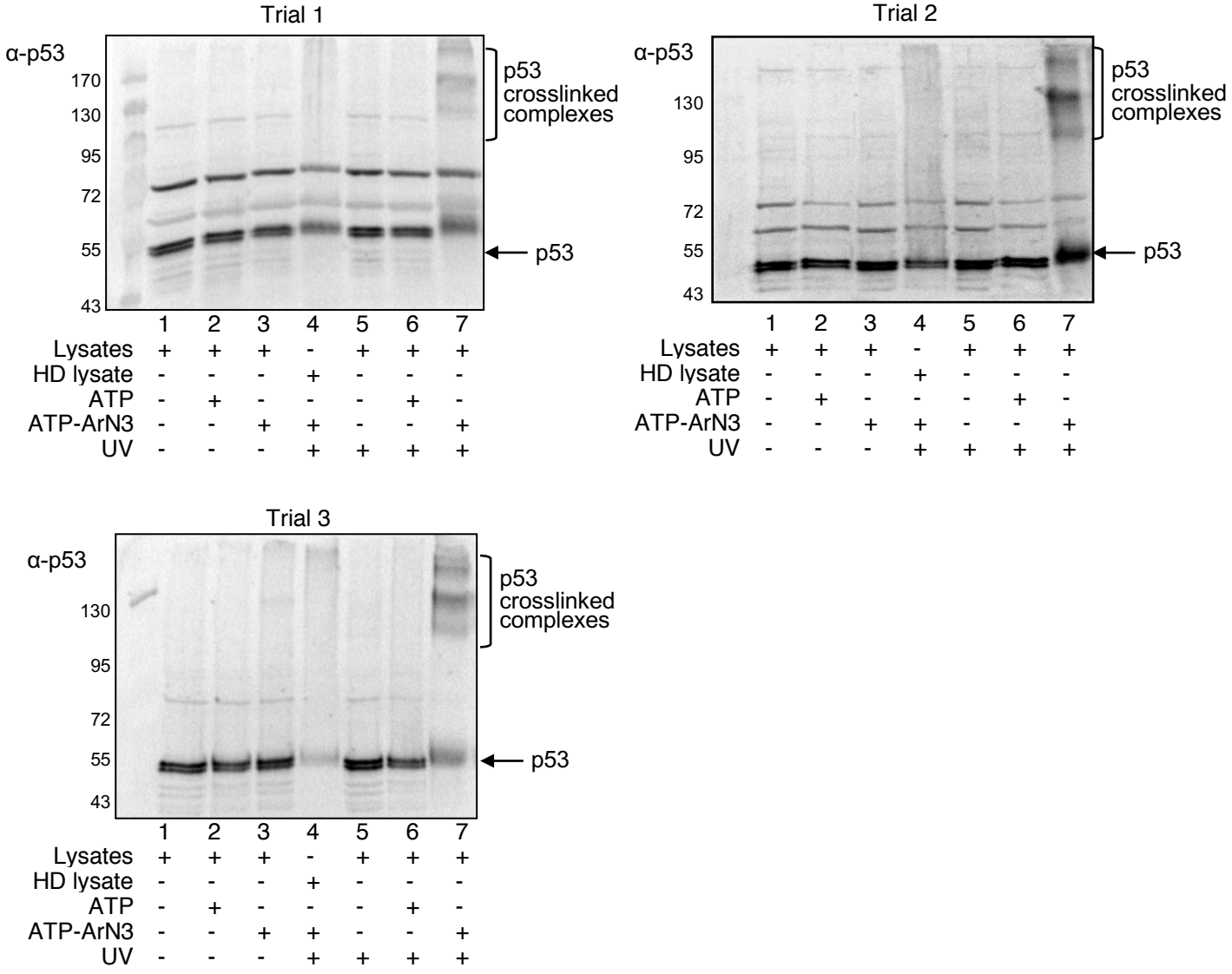

Figure S2. Kinase-catalyzed labeling reactions with p53. Kinase-catalyzed crosslinking reactions were performed using the indicated reaction components, followed by SDS-PAGE separation and visualization with a p53 antibody. HD lysates indicates heat-denatured lysates (lane 4). The high molecular weight crosslinked bands are indicated as p53 crosslinked complexes, and the p53 protein is also indicated with an arrow. Three trials are shown here, with the full gel image of Figure 2A in the manuscript provided as Trial 1.

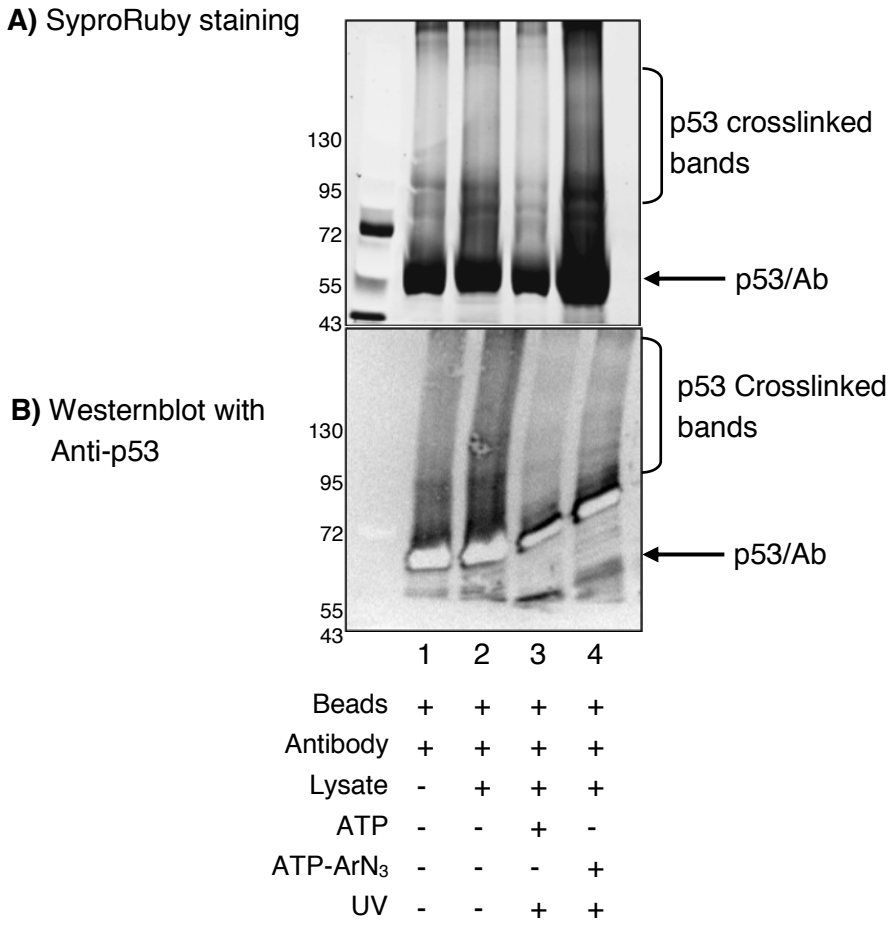

Figure S3: Immunoprecipitation (IP) of p53-Crosslinked Complexes using a mouse monoclonol antibody. Photocrosslinking reactions were performed by incubating the reaction components under UV as indicated under each lane at 30 °C for 2 hrs, followed by immunoprecipitation with p53 mouse monoclonal antibody, SDS-PAGE separation, and visualization with SyproRuby protein staining (top), or the rabbit polyclonol p53 antibody (bottom). ATP-ArN_3 (10 mM) and nutlin-treated RKO cell lysates were used in each reaction. The high molecular weight crosslinked complexes are indicated as p53 crosslinked bands. The 53 kDa band of p53 protein is indicated with an arrow. Due to co-migration of the heavy chain of the antibody from the IP with p53, the presence of antibody (Ab) is also indicated at the arrow. A molecular weight marker is shown on the far-left side of the gel images. This K-CLIP trial using rabbit polycolonal antibody for IP represents trial 2, with the first trial using mouse monoclonal antibody shown in Figure 2B of the manuscript. Both trials were analyzed by LC-MS/MS to identify p53-crosslinked proteins.

Table S1: Proteins identified by LC-MS/MS analysis in the p53 K-CLIP experiment[a]

No.	Identified Protein	Gene name	MW (kDa)	# of Peptides			
				A	B	C	D
1	Cytoplasmic dynein 1 heavy chain 1	DYHC1_HUMAN	532	0	5	0	62
2	DNA-dependent protein kinase catalytic subunit	PRKDC_HUMAN	469	0	7	0	47
3	Filamin-B	FLNB_HUMAN	278	0	11	0	31
4	Isoleucine--tRNA ligase, cytoplasmic, IARS	SYIC_HUMAN	145	0	4	0	36
5	Transcription intermediary factor 1-beta, TRIM28	TIF1B_HUMAN	89	0	11	0	29
6	Leucine--tRNA ligase, cytoplasmic, LARS	SYLC_HUMAN	134	0	7	0	32
7	Fatty acid synthase	FAS_HUMAN	273	0	3	0	35
8	X-ray repair cross-complementing protein 6	XRCC6_HUMAN	70	0	2	0	31
9	Poly [ADP-ribose] polymerase 1	PARP1_HUMAN	113	0	4	0	29
10	26S proteasome non-ATPase regulatory subunit 2	PSMD2_HUMAN	100	0	5	0	24
11	Polypyrimidine tract-binding protein 1	PTBP1_HUMAN	57	0	9	0	20
12	Hexokinase-1	HXK1_HUMAN	102	0	5	0	23
13	Heterogeneous nuclear ribonucleoprotein U	HNRPU_HUMAN	91	0	4	0	24
14	Coatomer subunit beta	COPB_HUMAN	107	0	7	0	20
15	Myosin-9	MYH9_HUMAN	227	0	2	0	25
16	Lon protease homolog, mitochondrial	LONM_HUMAN	106	0	3	0	23
17	Gamma-interferon-inducible protein 16	IF16_HUMAN	88	0	4	0	20
18	Translational activator GCN1	GCN1L_HUMAN	293	0	1	0	22
19	Eukaryotic translation initiation factor 3 subunit C	EIF3C_HUMAN	105	0	3	0	20
20	Ras GTPase-activating-like protein	IQGA1_HUMAN	189	0	2	0	20
21	X-ray repair cross-complementing protein 5	XRCC5_HUMAN	83	0	2	0	20
22	Sarcoplasmic/endoplasmic reticulum calcium ATPase 2	AT2A2_HUMAN	115	0	3	0	17
23	ATP-dependent RNA helicase	DDX3X_HUMAN	73	0	4	0	16
24	Importin-4	IPO4_HUMAN	119	0	3	0	16
25	Exportin-1	XPO1_HUMAN	123	0	2	0	17
26	Bifunctional glutamate/proline--tRNA ligase, EPRS	SYEP_HUMAN	171	0	3	0	16
27	ATP-dependent RNA helicase DDX1	DDX1_HUMAN	82	0	5	0	14
28	Dolichyl-diphosphooligosaccharide--protein	RPN1_HUMAN	69	0	4	0	15
29	CAD protein	PYR1_HUMAN	243	0	2	0	17
30	Heat shock 70 kDa protein 4L, HSPA4	HS74L_HUMAN	95	0	6	0	13
31	pre-mRNA-splicing factor ATP-dependent RNA helicase	DHX15_HUMAN	91	0	3	0	15
32	U5 small nuclear ribonucleoprotein 200 kDa helicase	U520_HUMAN	245	0	3	0	14
33	Programmed cell death 6-interacting protein	PDC6I_HUMAN	96	0	3	0	14
34	Sodium/potassium-transporting ATPase subunit alpha1	AT1A1_HUMAN	113	0	2	0	15
35	Myb-binding protein 1A, MYBBP1A	MBB1A_HUMAN	149	0	1	0	15
36	Calpain-2 catalytic subunit	CAN2_HUMAN	80	0	4	0	12
37	Coronin-1C OS=Homo sapiens	COR1C_HUMAN	53	0	10	0	6
38	ATP-dependent RNA helicase A	DHX9_HUMAN	141	0	1	0	15
39	Trifunctional enzyme subunit alpha, HADHA	ECHA_HUMAN	83	0	3	0	13
40	FACT complex subunit SSRP1	SSRP1_HUMAN	81	0	5	0	10
41	ADP/ATP translocase 2, SLC25A5	ADT2_HUMAN	33	0	3	0	12
42	Talin-1	TLN1_HUMAN	270	0	2	0	13
43	Arginine--tRNA ligase, cytoplasmic	SYRC_HUMAN	75	0	2	0	13
44	Dolichyl-diphosphooligosaccharide--protein	RPN2_HUMAN	69	0	5	0	10

45	Coatomer subunit alpha	COPA_HUMAN	138	0	1	0	13
46	Matrin-3	MATR3_HUMAN	95	0	2	0	12
47	Trifunctional purine biosynthetic protein adenosine-3	PUR2_HUMAN	108	0	3	0	11
48	General vesicular transport factor p115 SV=2	USO1_HUMAN	108	0	2	0	12
49	Importin-5	IPO5_HUMAN	124	0	2	0	11
50	Extended synaptotagmin-1	ESYT1_HUMAN	123	0	3	0	10
51	N-acetyltransferase 10	NAT10_HUMAN	116	0	2	0	11
52	Coatomer subunit gamma-1	COPG1_HUMAN	98	0	3	0	10
53	Alanine--tRNA ligase, cytoplasmic, AARS	SYAC_HUMAN	107	0	3	0	10
54	Splicing factor 3B subunit 3	SF3B3_HUMAN	136	0	2	0	10
55	Protein disulfide-isomerase A6	PDIA6_HUMAN	48	0	1	0	11
56	Kinesin-1 heavy chain OS=Homo sapiens, KIF5B	KINH_HUMAN	110	0	3	0	8
57	Squamous cell carcinoma antigen recognized by T-cells	SART3_HUMAN	110	0	2	0	9
58	26S proteasome non-ATPase regulatory subunit 3	PSMD3_HUMAN	61	0	7	0	4
59	General transcription factor II-I	GTF2I_HUMAN	112	0	1	0	9
60	Importin subunit beta-1	IMB1_HUMAN	97	0	1	0	9
61	DNA replication licensing factor MCM3	MCM3_HUMAN	91	0	2	0	8
62	Transitional endoplasmic reticulum ATPase, VCP	TERA_HUMAN	89	0	1	0	9
63	DNA replication licensing factor MCM6	MCM6_HUMAN	93	0	1	0	9
64	ATP-dependent DNA helicase	RECQ1_HUMAN	73	0	1	0	9
65	Cofilin-1	COF1_HUMAN	19	0	1	0	9
66	ADP/ATP translocase 3, SLC25A6	ADT3_HUMAN	33	0	1	0	8
67	Niban-like protein 1	NIBL1_HUMAN	84	0	1	0	8
68	Monofunctional C1-tetrahydrofolate synthase,	C1TM_HUMAN	106	0	3	0	6
69	Nucleoprotein TPR	TPR_HUMAN	267	0	1	0	8
70	Dynamin-like 120 kDa protein, mitochondrial	OPA1_HUMAN	112	0	2	0	7
71	Copine-1	CPNE1_HUMAN	59	0	5	0	4
72	Heterogeneous nuclear ribonucleoprotein R	HNRPR_HUMAN	71	0	1	0	8
73	DBIRD complex subunit KIAA1967	K1967_HUMAN	103	0	1	0	7
74	Exosome complex exonuclease RRP44, DIS3	RRP44_HUMAN	109	0	1	0	7
75	tRNA (cytosine(34)-C(5))-methyltransferase	NSUN2_HUMAN	86	0	1	0	7
76	26S proteasome non-ATPase regulatory subunit 1	PSMD1_HUMAN	106	0	3	0	5
77	Apoptosis-inducing factor 1, mitochondrial	AIFM1_HUMAN	67	0	4	0	4
78	Stress-induced-phosphoprotein 1	STIP1_HUMAN	63	0	2	0	6
79	Non-POU domain-containing octamer-binding protein	NONO_HUMAN	54	0	2	0	5
80	Asparagine synthetase [glutamine-hydrolyzing]	ASNS_HUMAN	64	0	3	0	4
81	NADPH:adrenodoxin oxidoreductase, mitochondrial	ADRO_HUMAN	54	0	4	0	3
82	Neutral amino acid transporter B(0)	AAAT_HUMAN	57	0	1	0	6
83	Dynamin-2 SV=2	DYN2_HUMAN	98	0	1	0	6
84	Peptidyl-prolyl cis-trans isomerase FKBP4	FKBP4_HUMAN	52	0	5	0	2
85	Far upstream element-binding protein 2, KHSRP	FUBP2_HUMAN	73	0	1	0	6
86	Serine/threonine-protein phosphatase 2A, PPP2R1A	2AAA_HUMAN	65	0	1	0	6
87	Oxysterol-binding protein-related protein 8	OSBL8_HUMAN	101	0	2	0	5
88	CTP synthase 1, CTPS1	PYRG1_HUMAN	67	0	1	0	6
89	RuvB-like 1	RUVB1_HUMAN	50	0	1	0	6
90	RNA-binding protein 12	RBM12_HUMAN	97	0	1	0	6
91	Splicing factor 3A subunit 1	SF3A1_HUMAN	89	0	1	0	6

92	Valine--tRNA ligase, VARS	SYVC_HUMAN	140	0	1	0	6
93	Methionine--tRNA ligase, cytoplasmic, MARS	SYMC_HUMAN	101	0	2	0	5
94	Fascin	FSCN1_HUMAN	55	0	2	0	4
95	Aspartate--tRNA ligase, cytoplasmic, DARS	SYDC_HUMAN	57	0	2	0	4
96	Metastasis-associated protein MTA2	MTA2_HUMAN	75	0	1	0	5
97	Far upstream element-binding protein 3	FUBP3_HUMAN	62	0	3	0	3
98	Glutamine--tRNA ligase, QARS	SYQ_HUMAN	88	0	1	0	5
99	Protein unc-45 homolog A	UN45A_HUMAN	103	0	1	0	5
100	26S protease regulatory subunit 4, PSMC1	PRS4_HUMAN	49	0	1	0	5
101	MMS19 nucleotide excision repair protein homolog	MMS19_HUMAN	113	0	2	0	3
102	Drebrin, DBN1	DREB_HUMAN	71	0	1	0	4
103	Tyrosine--tRNA ligase, cytoplasmic, YARS	SYYC_HUMAN	59	0	4	0	1
104	Phenylalanine--tRNA ligase alpha subunit, FARSSV	SYFA_HUMAN	58	0	2	0	3
105	Coatomer subunit beta'	COPB2_HUMAN	102	0	1	0	4
106	Heterogeneous nuclear ribonucleoprotein L	HNRPL_HUMAN	64	0	3	0	2
107	Ubiquitin-protein ligase E3C	UBE3C_HUMAN	124	0	1	0	4
108	Hexokinase-2, HK2	HXK2_HUMAN	102	0	1	0	3
109	5'-3' exoribonuclease 2	XRN2_HUMAN	109	0	2	0	2
110	Probable ATP-dependent RNA helicase DDX41	DDX41_HUMAN	70	0	2	0	2
111	Caprin	CAPR1_HUMAN	78	0	1	0	3
112	Protein LYRIC, MTDH	LYRIC_HUMAN	64	0	1	0	3
113	Serine/threonine-protein kinase MRCK beta	MRCKB_HUMAN	194	0	3	0	1
114	Desmocollin-1	DSC1_HUMAN	100	0	1	0	3
115	Adenylyl cyclase-associated protein 1	CAP1_HUMAN	52	0	1	0	3
116	Interferon-induced, double-stranded RNA-activated	E2AK2_HUMAN	62	0	1	0	3
117	DNA replication licensing factor MCM7	MCM7_HUMAN	81	0	1	0	3
118	Importin-9	IPO9_HUMAN	116	0	1	0	2
119	Exportin-7	XPO7_HUMAN	124	0	1	0	2
120	Importin-11	IPO11_HUMAN	113	0	2	0	1
121	Zymogen granule protein 16 homolog B	ZG16B_HUMAN	23	0	1	0	2
122	Alpha-aminoadipic semialdehyde synthase,	AASS_HUMAN	102	0	1	0	2
123	Coatomer subunit delta, ARCN1	COPD_HUMAN	57	0	1	0	2
124	DnaJ homolog subfamily C member 2	DNJC2_HUMAN	72	0	1	0	2
125	Dihydrolipoyllysine-residue succinyltransferase	ODO2_HUMAN	49	0	2	0	1
126	Pentatricopeptide repeat domain-containing protein 3	PTCD3_HUMAN	79	0	1	0	2
127	SCY1-like protein 2	SCYL2_HUMAN	104	0	1	0	2
128	Protein VAC14 homolog	VAC14_HUMAN	88	0	1	0	2

[a]This table catalogs the number of unique peptides identified after K-CLIP. Lettered columns on right display the number of unique peptides observed for the indicated proteins in uncrosslinked (A and C) or crosslinked (B and D) K-CLIP reactions with a rabbit (A and B) or mouse (C and D) p53 antibody immunoprecipitation. The parameters in Scaffold used in this analysis were set to a 90% protein threshold, 99.9% peptide threshold, with the minimum number of peptides set to 1. Only proteins observed in crosslinked reactions (columns B and D), but not uncrosslinked reactions (columns A and C) are displayed as hits. Proteins highlighted in yellow are kinases included in Table 1. Proteins highlighted in green are direct interacting proteins (Figure 5B) and proteins highlighted in blue are indirect associated proteins (Figure 5A) of p53.

P53_HUMAN (100%), 43,653.4 Da
Cellular tumor antigen p53 OS=Homo sapiens GN=TP53 PE=1 SV=4
7 exclusive unique peptides, 7 exclusive unique spectra, 14 total spectra, 85/393 amino acids (22% coverage)

M E E P Q S D P S V E P P L S Q E T F S D L W K L L P E N N V L S P L P S Q A M D D L M L S P D D I
E Q W F T E D P G P D E A P R M P E A A P P V A P A P A A P T P A A P A P A P S W P L S S S V P S Q
K T Y Q G S Y G F R L G F L H S G T A K S V T C T Y S P A L N K M F C Q L A K T C P V Q L W V D S T
P P P G T R V R A M A I Y K Q S Q H M T E V V R R C P H H E R C S D S D G L A P P Q H L I R V E G N
L R V E Y L D D R N T F R H S V V V P Y E P P E V G S D C T T I H Y N Y M C N S S C M G G M N R R P
I L T I I T L E D S S G N L L G R N S F E V R V C A C P G R D R R T E E E N L R K K G E P H H E L P
P G S T K R A L P N N T S S S P Q P K K P L D G E Y F T L Q I R G R E R F E M F R E L N E A L E L
K D A Q A G K E P G G S R A H S S H L K S K K G Q S T S R H K K L M F K T E G P D S D

Figure S4: Peptides for p53 identified by LC-MS/MS analysis using K-CLIP. Primary sequence of p53 is shown, with amino acids observed in the LC-MS/MS analysis highlighted in yellow. The parameters set were protein threshold- 90%, peptide threshold- 99.9%, with minimum number of peptides set to 1.

Peptide Sequence: (R)LGFLHSGTAK(S)

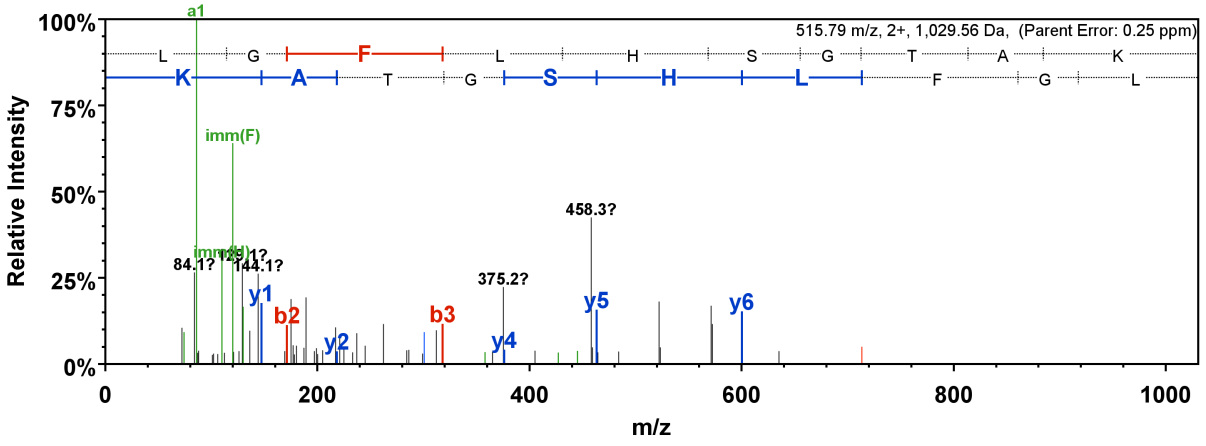

Peptide Sequence: (R)VEYLDDRNTFR(H)

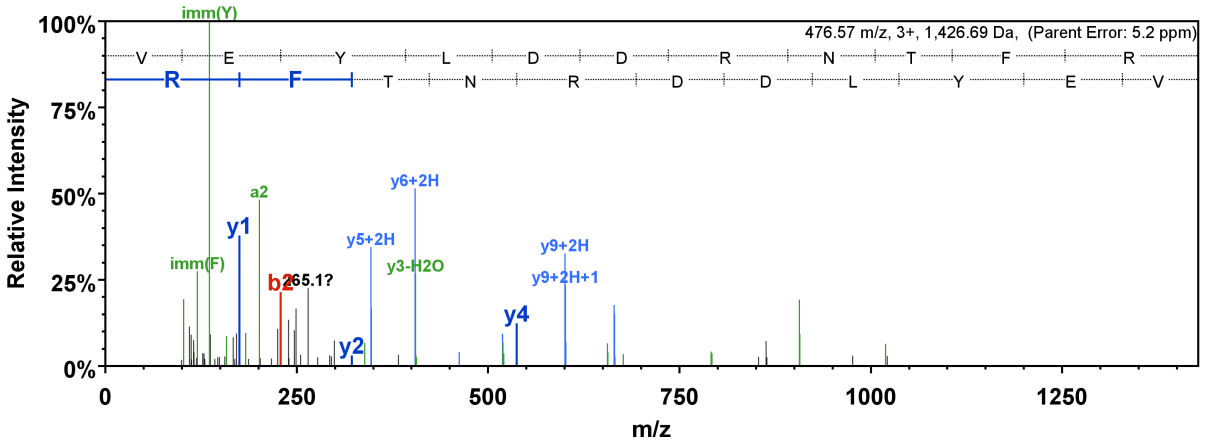

Peptide Sequence: (K)SVTcTYSPALNK(M)

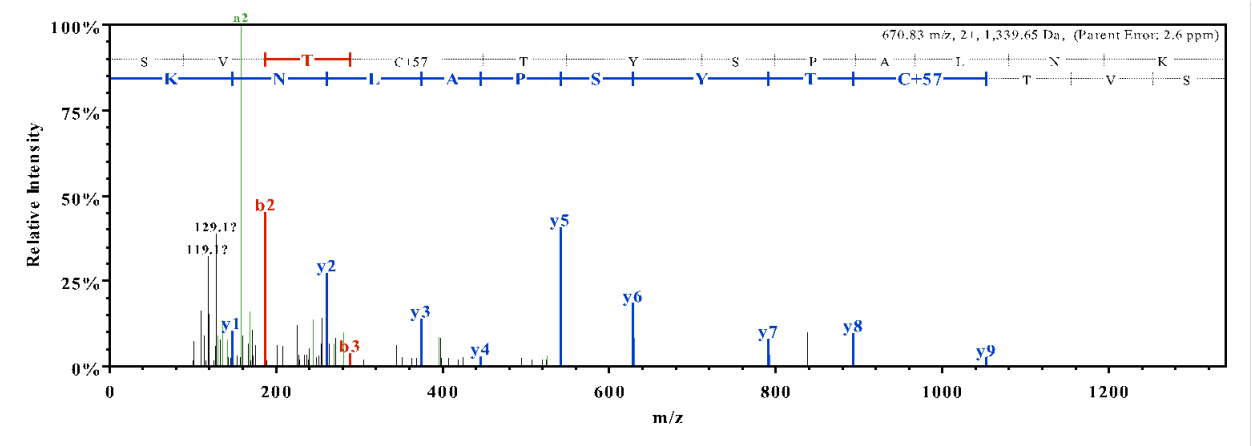

Peptide Sequence: (R)cSDSDGLAPPQHLIR(V)

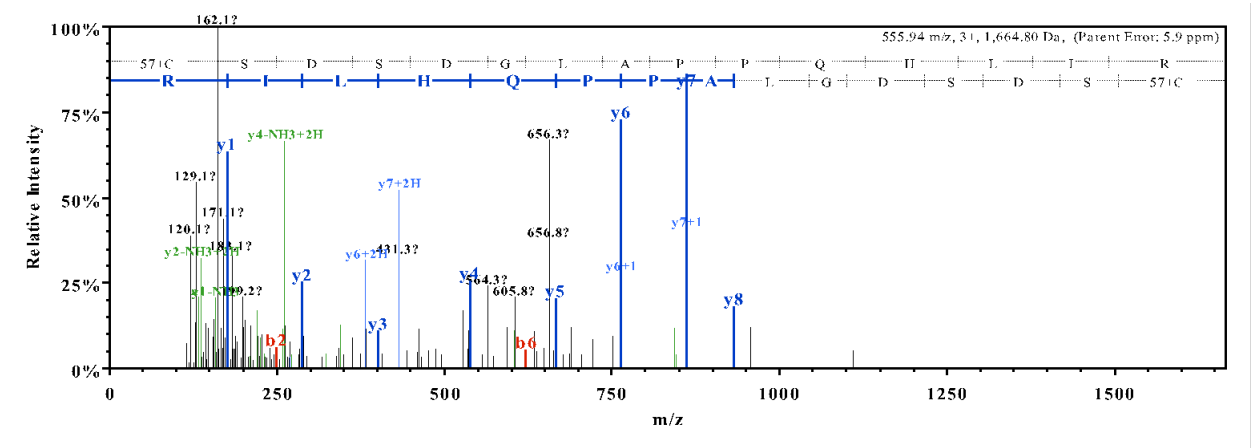

Peptide Sequence: (R)RPILTIITLEDSSGNLLGR(N)

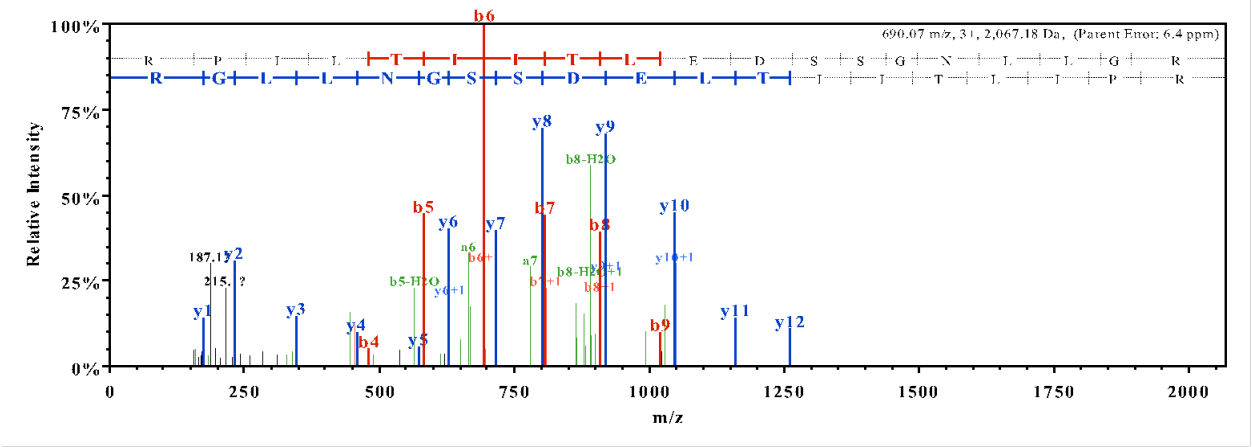

Peptide Sequence: (R)ALPNNTSSSPQPK(K)

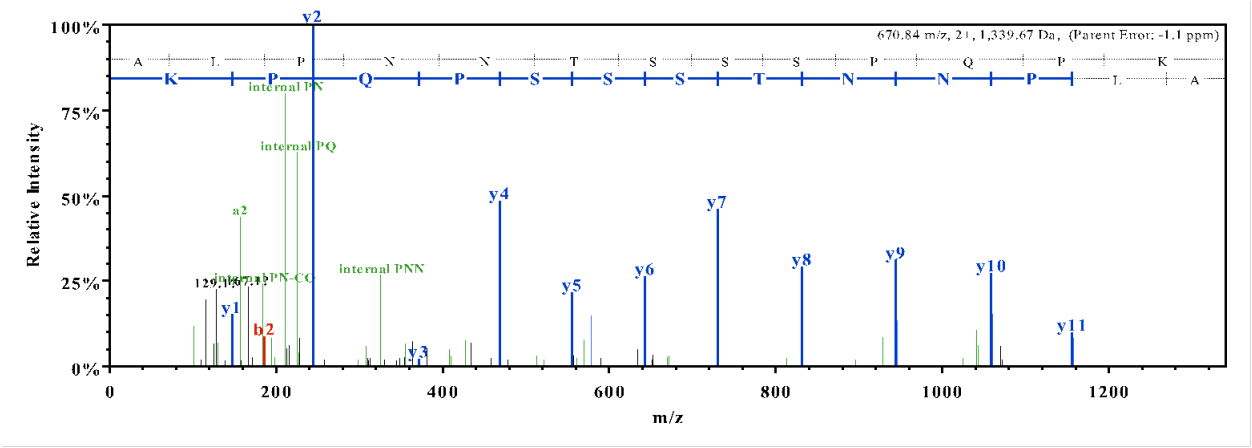

Peptide Sequence: (R)ELNEALELK(D)

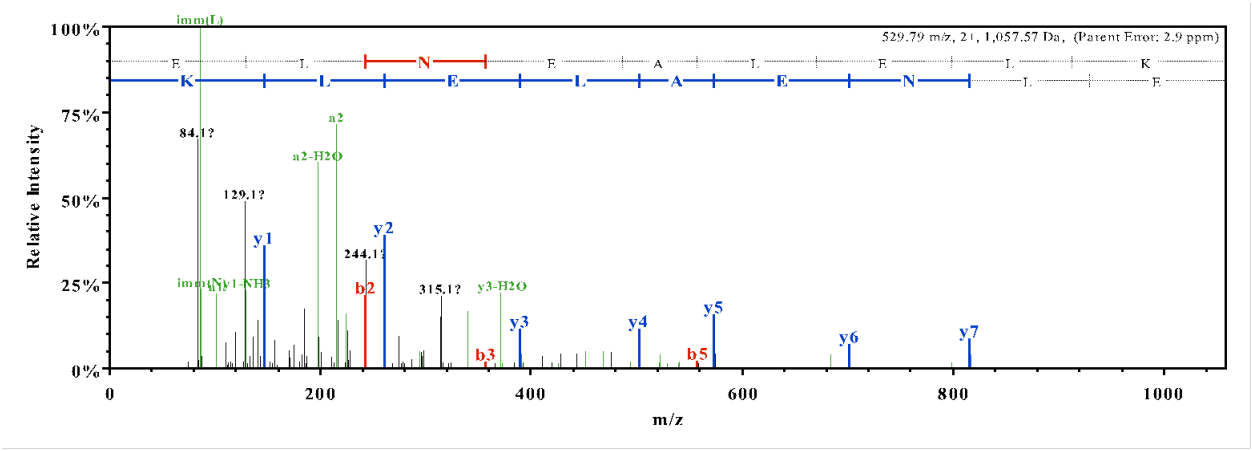

Peptide Sequence: (R)ELNEALELKDAQAGK(E)

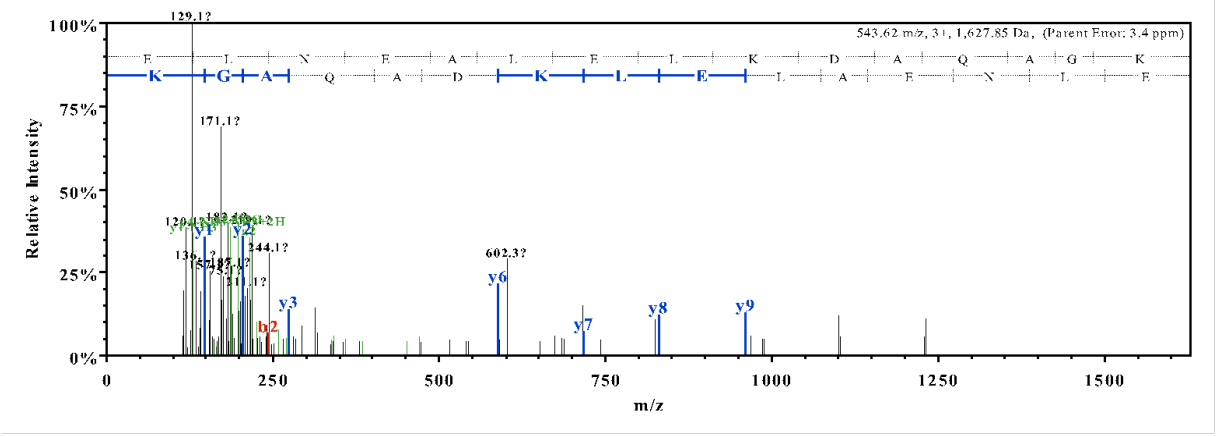

Figure S5: Annotated spectra of p53 peptides identified by LC-MS/MS analysis shown in Figure S4. A representation of the peptide fragments identified is shown with the peptide sequence on top of each spectrum.

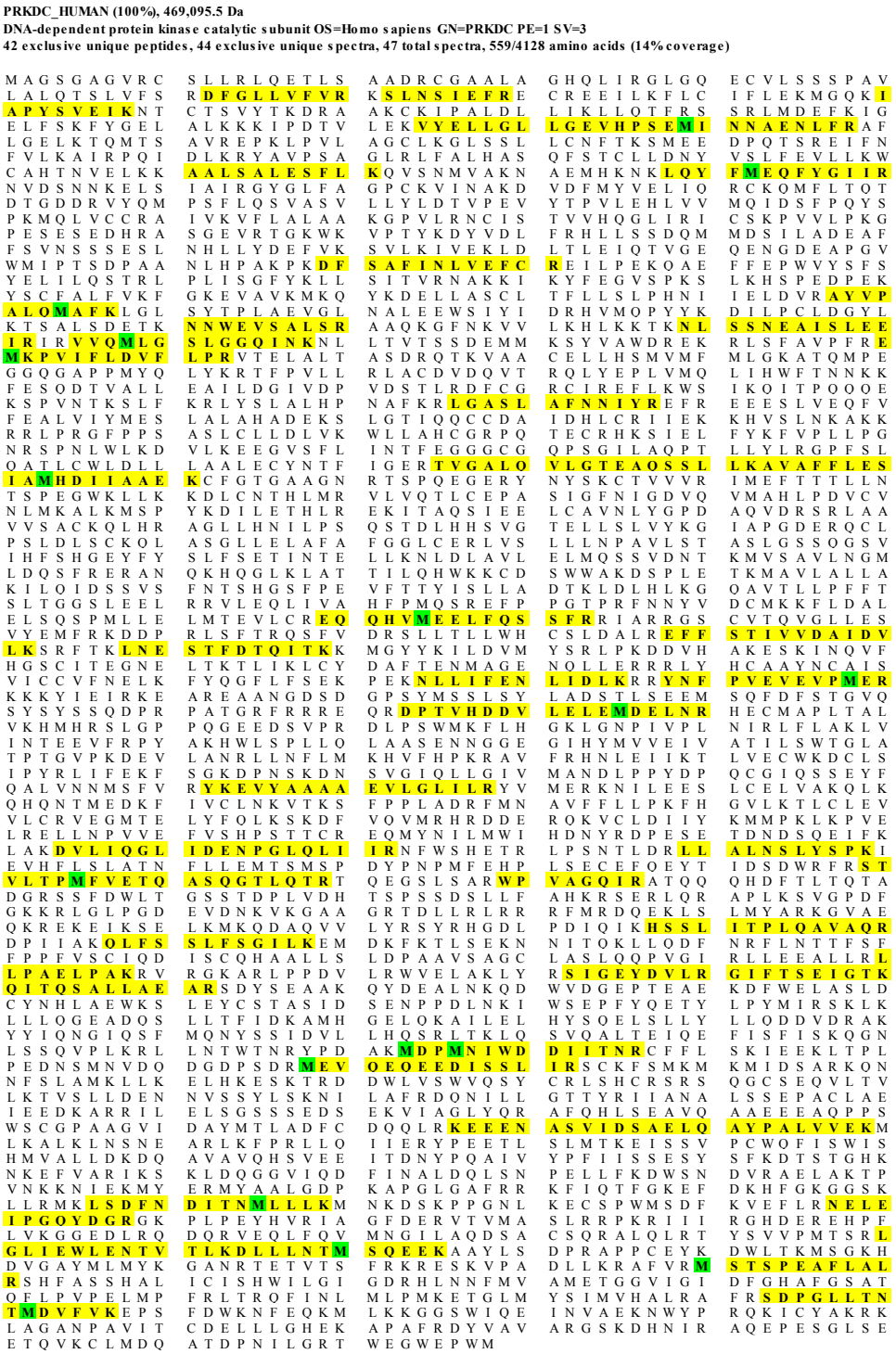

Figure S6: Peptides for DNA-PK identified by LC-MS/MS analysis using K-CLIP. The primary sequence of DNA-PK is shown, with amino acids observed in the LC-MS/MS analysis highlighted in yellow and modified amino acids are in green (phosphorylation (S or T) or oxidation (M)). The parameters set were protein threshold- 90%, peptide threshold- 99.9%, with minimum number of peptides set to 1.

Peptide Sequence: (R)DPTVHDDVLELEMDELNR(H)

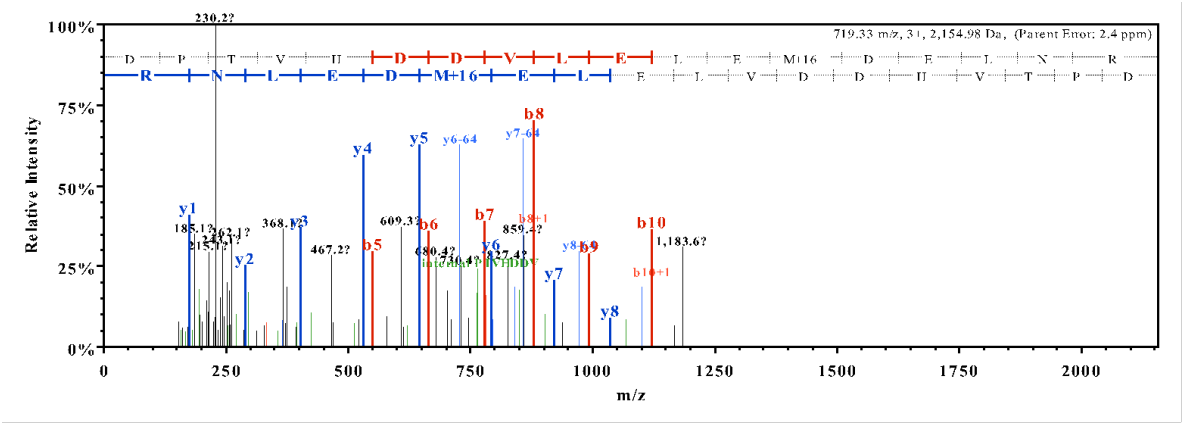

Peptide Sequence: (R)MEVQEQEEDISSLIR(S)

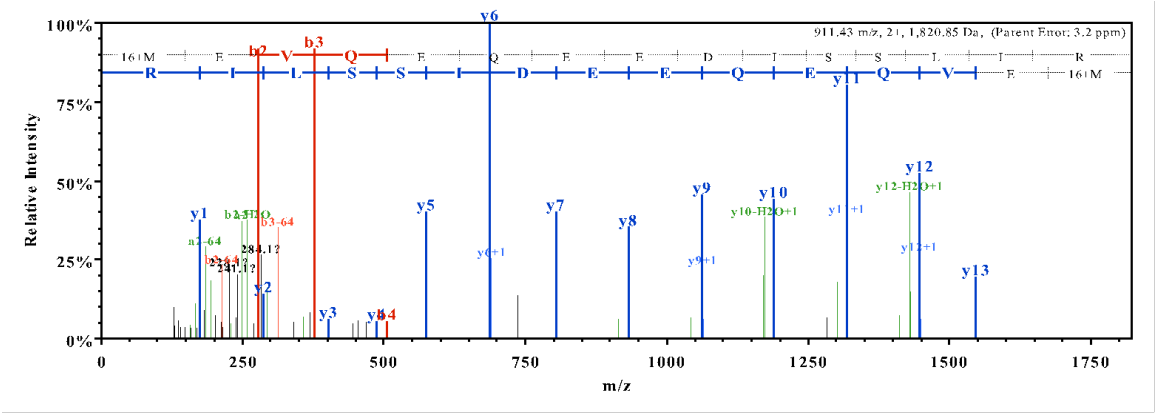

Peptide Sequence: (R)TVGALQVLGTEAQSSLLK(A)

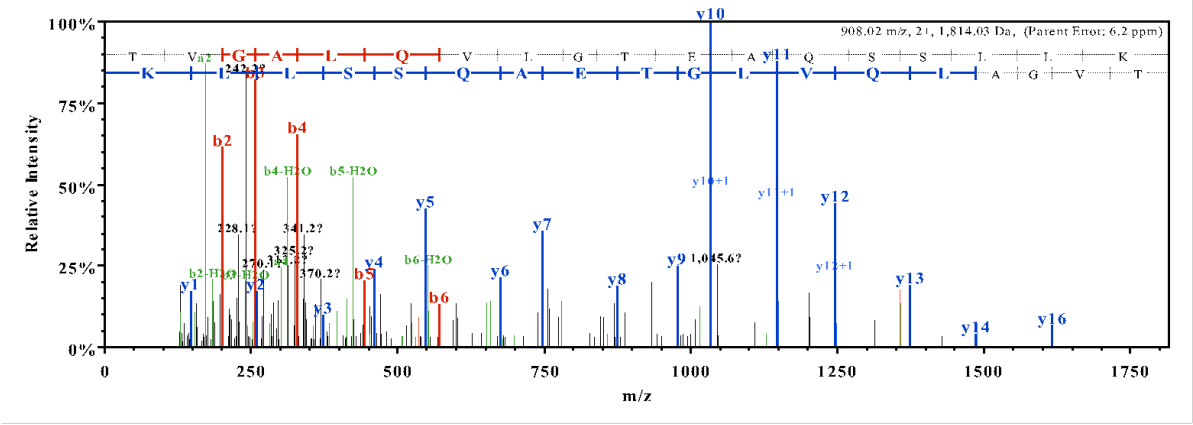

Figure S7: Annotated spectra of DNA-PK peptides identified by LC-MS/MS analysis, shown in Figure S6. Three illustrative spectra of peptide fragments identified are shown with the peptide sequence on top of each spectrum. Only three of 47 unique peptides are shown here for brevity.

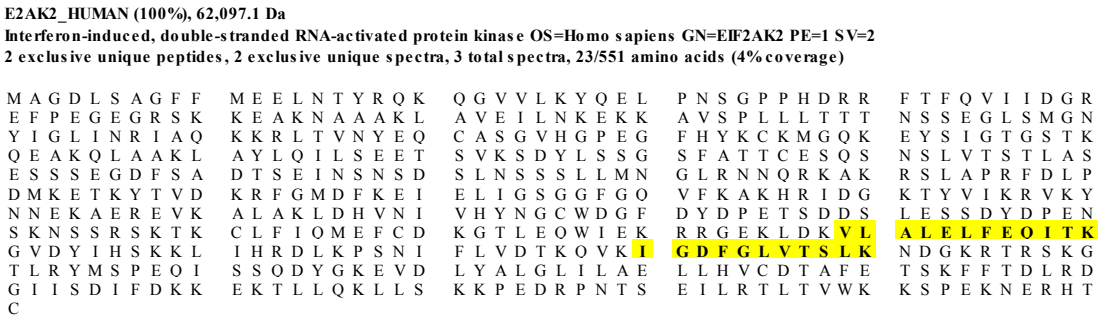

Figure S8: Peptides for PKR identified by LC-MS/MS analysis using K-CLIP. The primary sequence of PKR is shown, with amino acids observed in the MS/MS analysis highlighted in yellow. The parameters set were protein threshold- 90%, peptide threshold- 99.9%, with minimum number of peptides set to 1.

Peptide Sequence: (K)VLALELFEQITK(G)

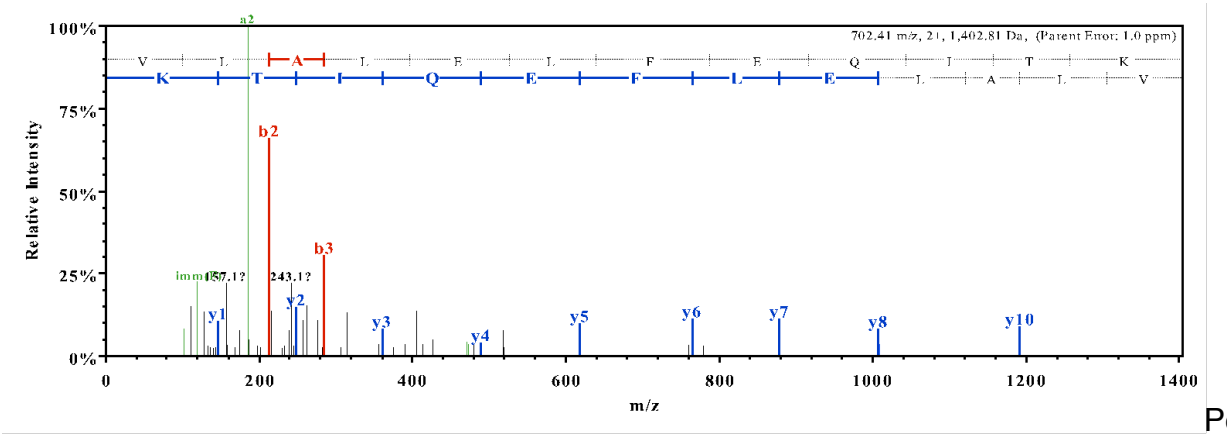

Peptide Sequence: (K)VLALELFEQITK(G)

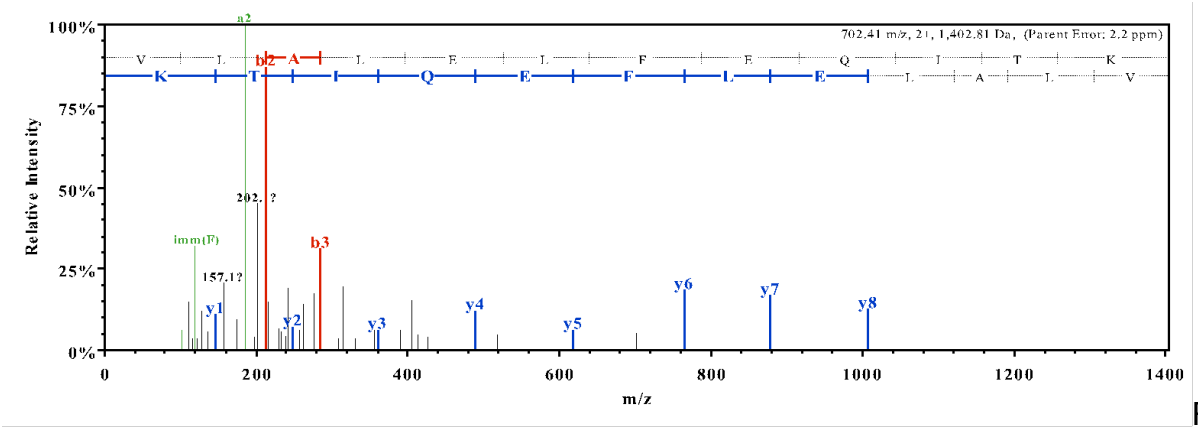

Peptide Sequence: (K)IGDFGLVTSLK(N)

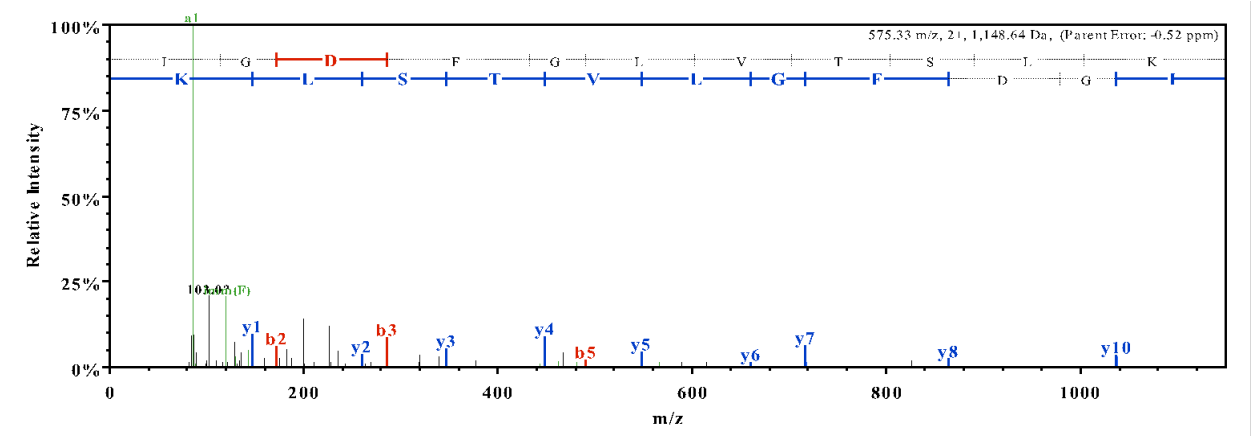

Figure S9: Annotated spectra of PKR peptides identified by LC-MS/MS analysis, shown in Figure S8. A representation of the peptide fragments identified is shown with the peptide sequence on top of each spectrum.

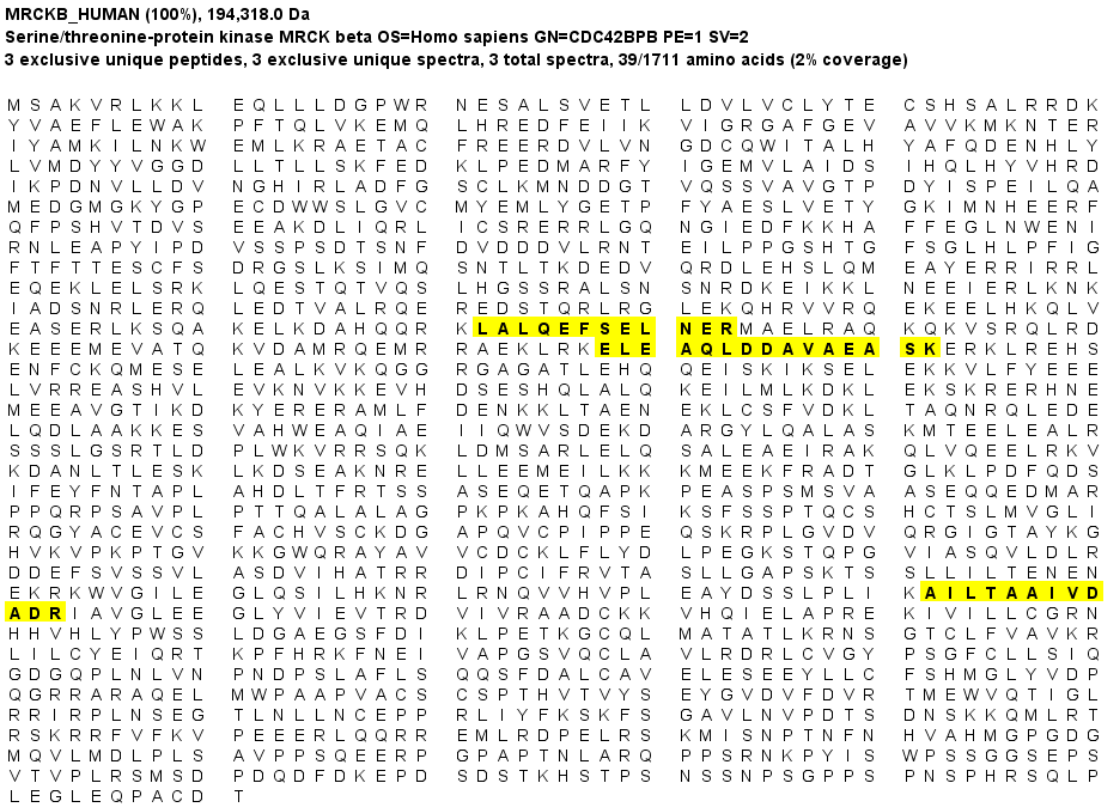

Figure S10: Peptides for MRCKβ identified by LC-MS/MS analysis using K-CLIP. The primary sequence of MRCKβ is shown, with amino acids observed in the MS/MS analysis highlighted in yellow. The parameters were, protein threshold- 90%, peptide threshold- 99.9%, with minimum number of peptides set to 1.

Peptide Sequence: (K)LALQEFSELNER(M)

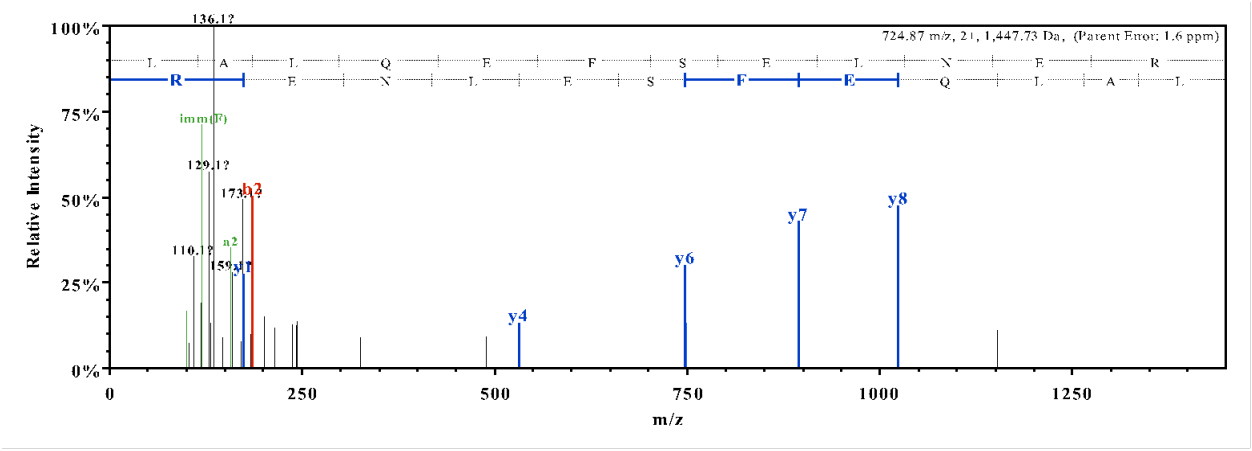

Peptide Sequence: (K)ELEAQLDDAVAEASK(E)

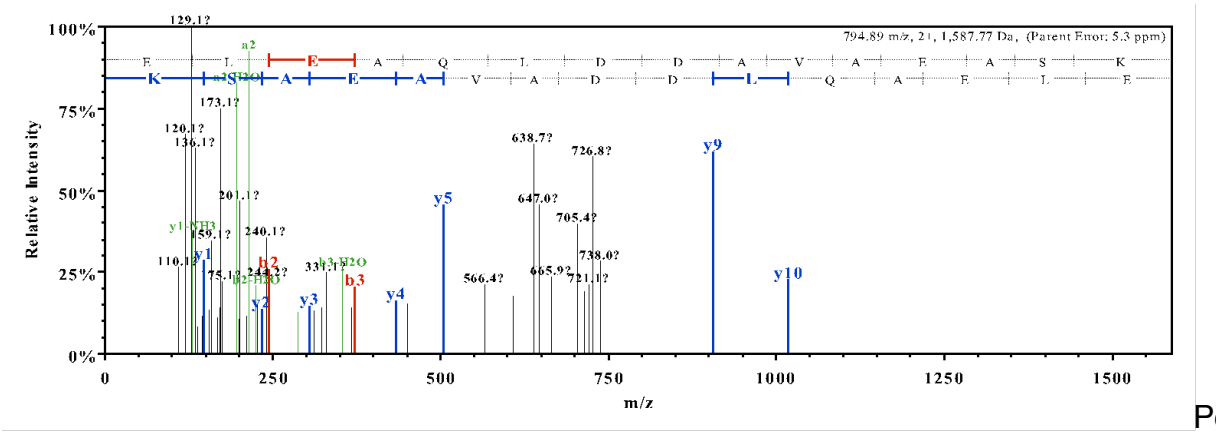

Peptide Sequence: (K)AILTAAIVDADR(I)

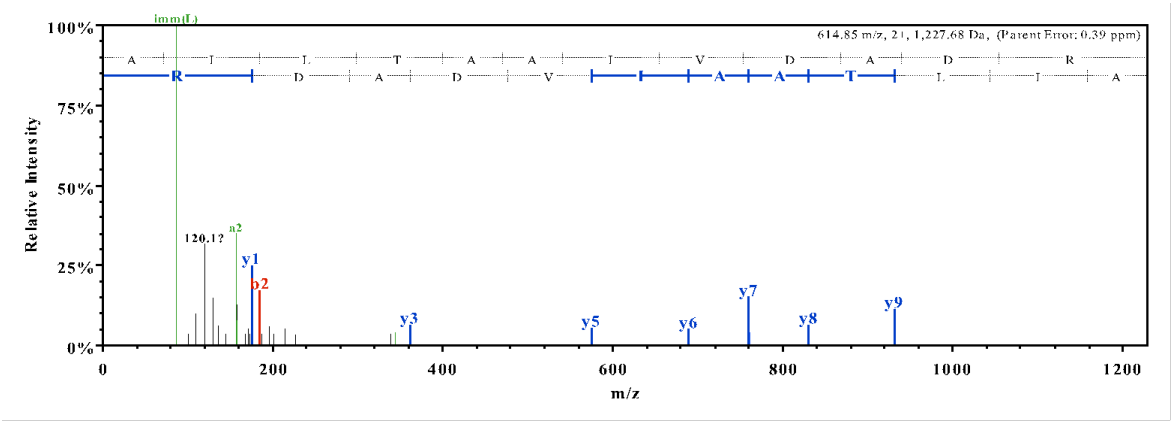

Figure S11: The annotated spectra of MRCKβ peptides identified by LC-MS/MS analysis, shown in Figure S10. A representation of the peptide fragments identified is shown with the peptide sequence on top of each spectrum.

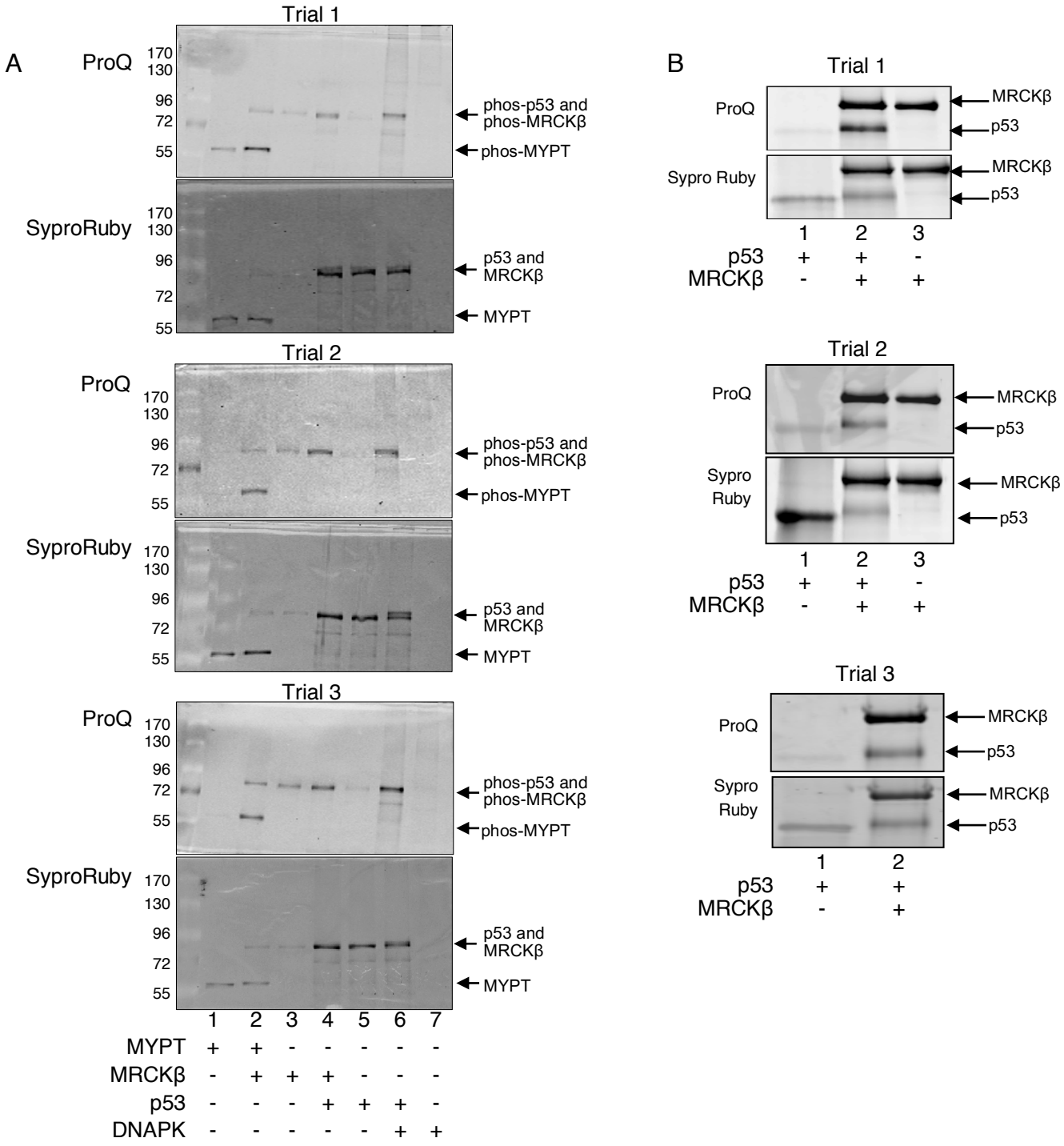

Figure S12: *In vitro* kinase assays with p53 and MRCKβ. A) Recombinant MYPT1 (0.5 μg, lanes 1-2) or p53 (0.5 μg, lanes 4-6) was incubated with recombinant MRCKβ (0.025 μg, lanes 2-4) or DNAPK (0.025 μg, lanes 6-7), along with ATP (4 mM). After separation by SDS-PAGE, phosphoproteins were visualized with ProQ Diamond stain (top) and total proteins were observed with SyproRuby stain (bottom). Three trials are shown here, with a cropped version of Trial 1 shown in Figure 3A of the manuscript. B) Large scale reactions- Recombinant p53 (5.5 μg, lanes 1-2) was incubated with recombinant MRCKβ (1.5 μg, lanes 2-3) and ATP (4 mM, all lanes), separated by SDS-PAGE, and visualized with ProQ Diamond phosphoprotein stain (top) or SyproRuby total protein stain (bottom). Autophosphorylation of MRCKβ was observed as a positive control for kinase activity. Bands corresponding to p53 and MRKCβ are indicated with arrows in all gel images. Three trials are shown here.

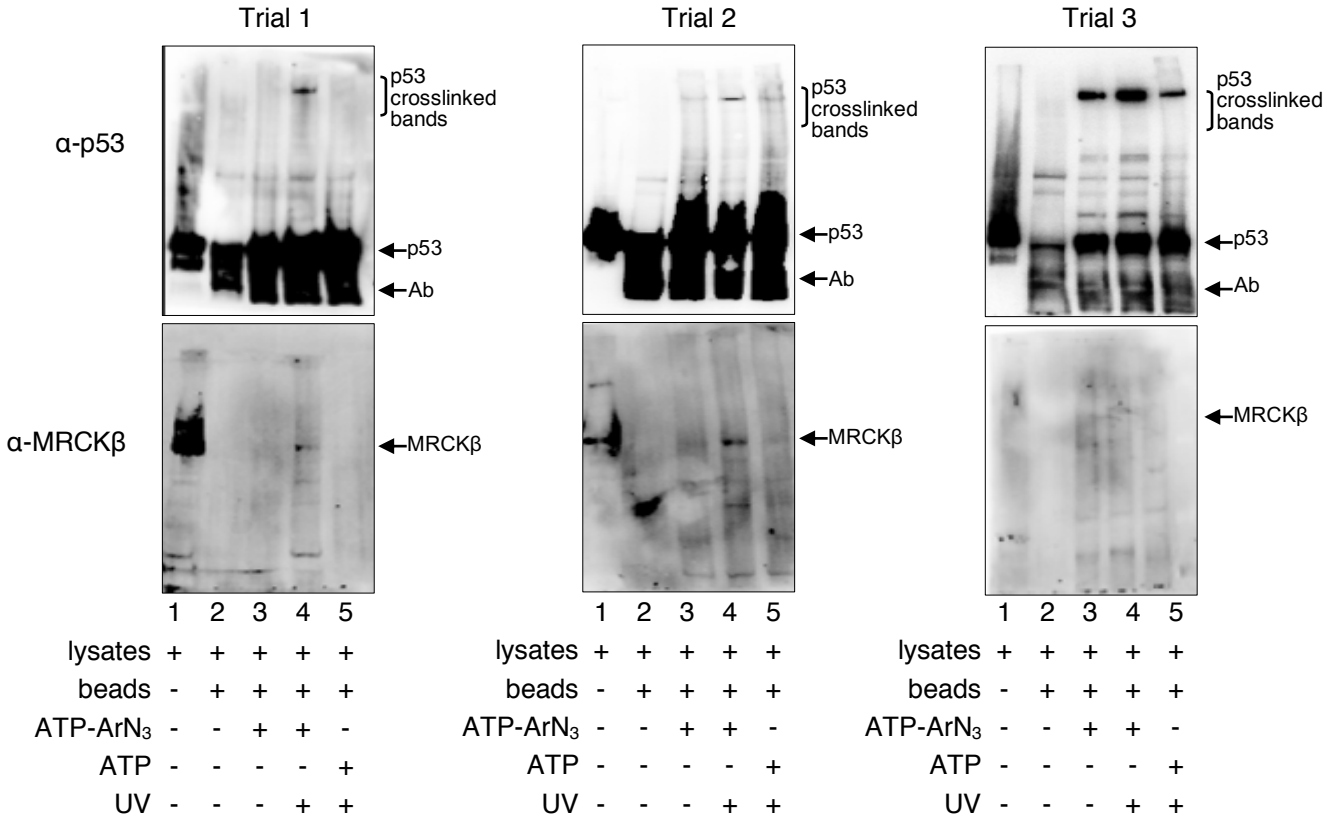

Figure S13: K-CLIP validates MRCKβ is a p53 kinase. K-CLIP was performed with RKO cell lysates after crosslinking using ATP-ArN_3 (lanes 3-4) or ATP (lane 5) either in the absence (lanes 1-3) or presence (lanes 4-5) of UV. After SDS-PAGE separation, both p53 (α-p53) and MRCKβ (α-MRCK) were visualized using Western blot analysis. Bands corresponding to p53 and MRKCβ are indicated with arrows in all gel images. Three trials are shown here, with a cropped version of Trial 1 shown in Figure 3B of the manuscript.

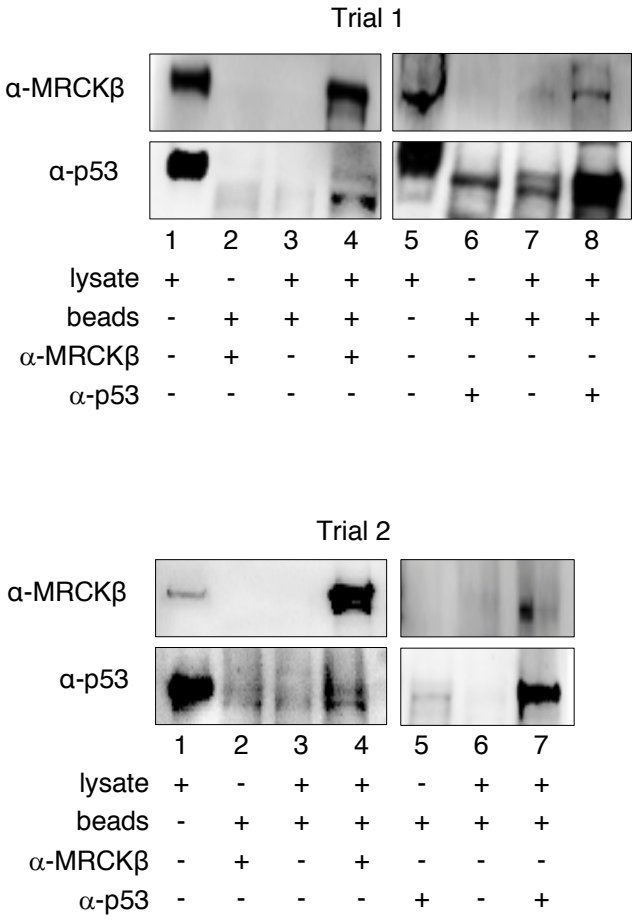

Figure S14: Coimmunoprecipitation studies of MRCKβ and p53. Coimmunoprecipitation was performed with RKO cell lysates and either MRCKβ or p53 antibodies, along with protein A/G agarose beads. After SDS-PAGE separation, Western blot analysis was performed with the MRCKβ (α-MRCK) or p53 (α-p53) antibodies. Two trials are shown here with a third trial shown in Figure 3C of the manuscript.

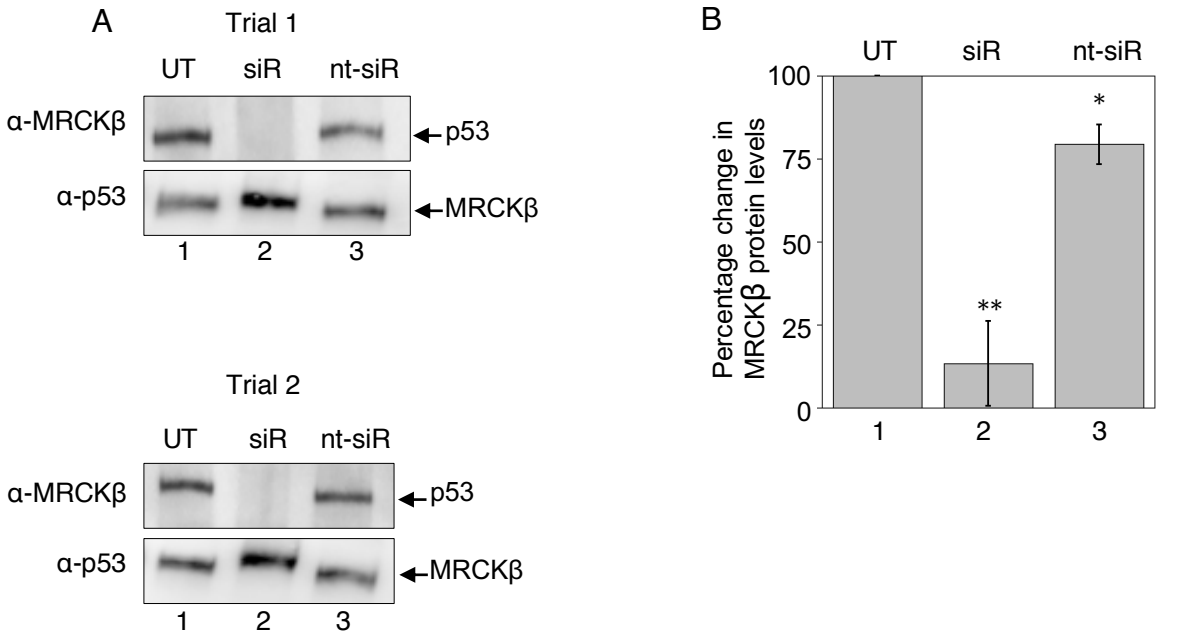

Figure S15: MRCKβ knockdown and p53 expression levels in RKO cells. A. RKO cells were untreated (UT, lane 1), treated with a pool of MRCKβ-targeting siRNA (siR, lane 2), or treated with a control non-targeting pool of siRNA (nt-siR, lane 3), along with a transfection reagent. After 72 hours at 37 °C, cells were harvested and lysed, before cellular proteins were separated by SDS-PAGE and visualized with both MRCKβ (α-MRCK) and p53 (α-p53) antibodies. Protein bands are indicated with arrows. Two trials are shown here, with another shown in Figure 3D of the manuscript. B) MRCKβ expression levels were quantified, with the mean and standard error shown. Data were analyzed by Prism software for statistical significance (*p = 0.0265 **p = 0.0025).

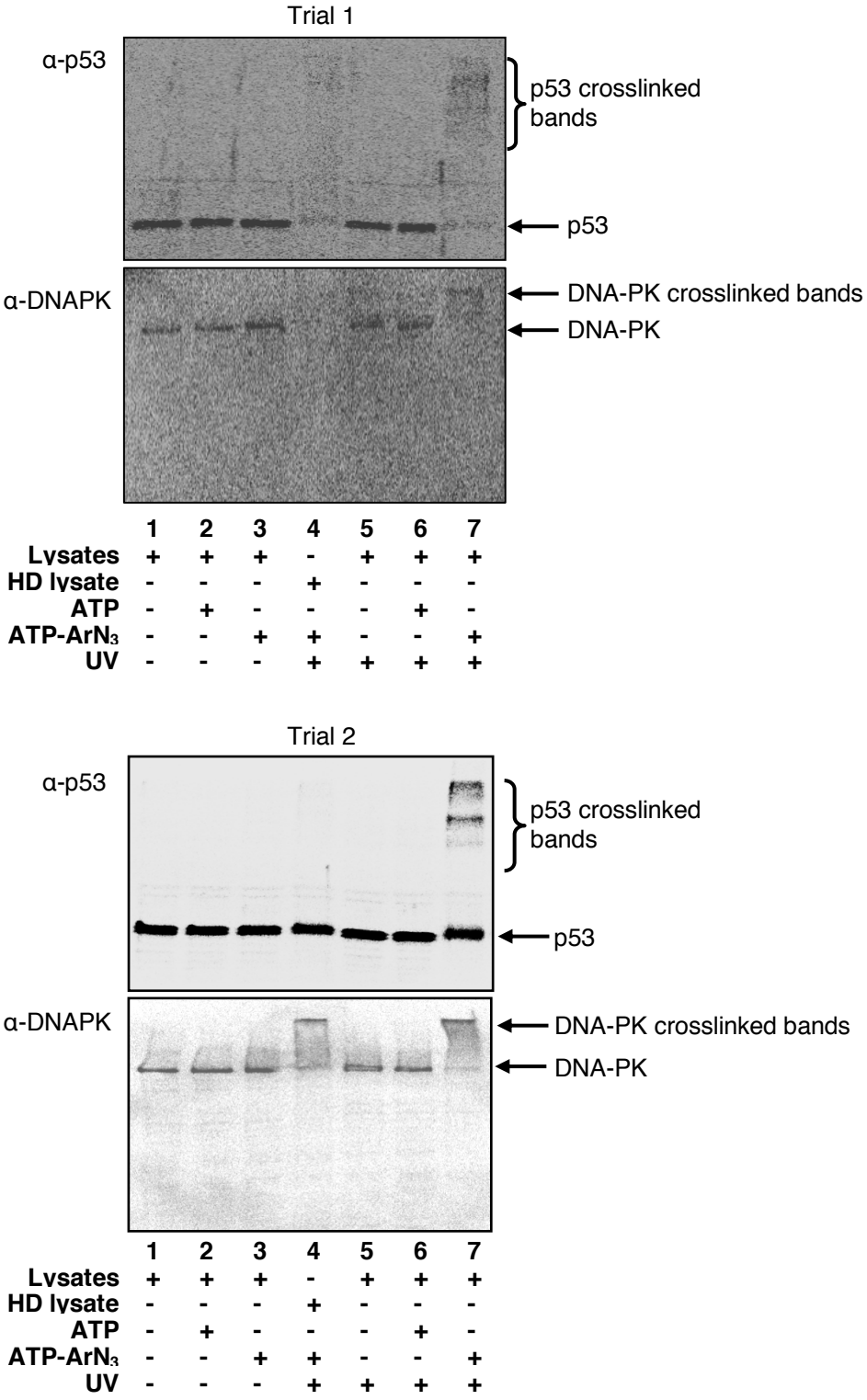

Figure S16: Kinase-catalyzed crosslinking validation reactions with DNAPK. Kinase-catalyzed crosslinking was performed using HeLa cell lysates (all lanes) and ATP-ArN_3 analog with or without UV, followed by SDS-PAGE separation and visualization with a p53 antibody (A and B, top) or a DNA-PK antibody (bottom). The high molecular weight crosslinked complexes of p53 and DNAPK are indicated with arrows. Two trials are shown here with a third trial shown in Figure 4A of the manuscript.

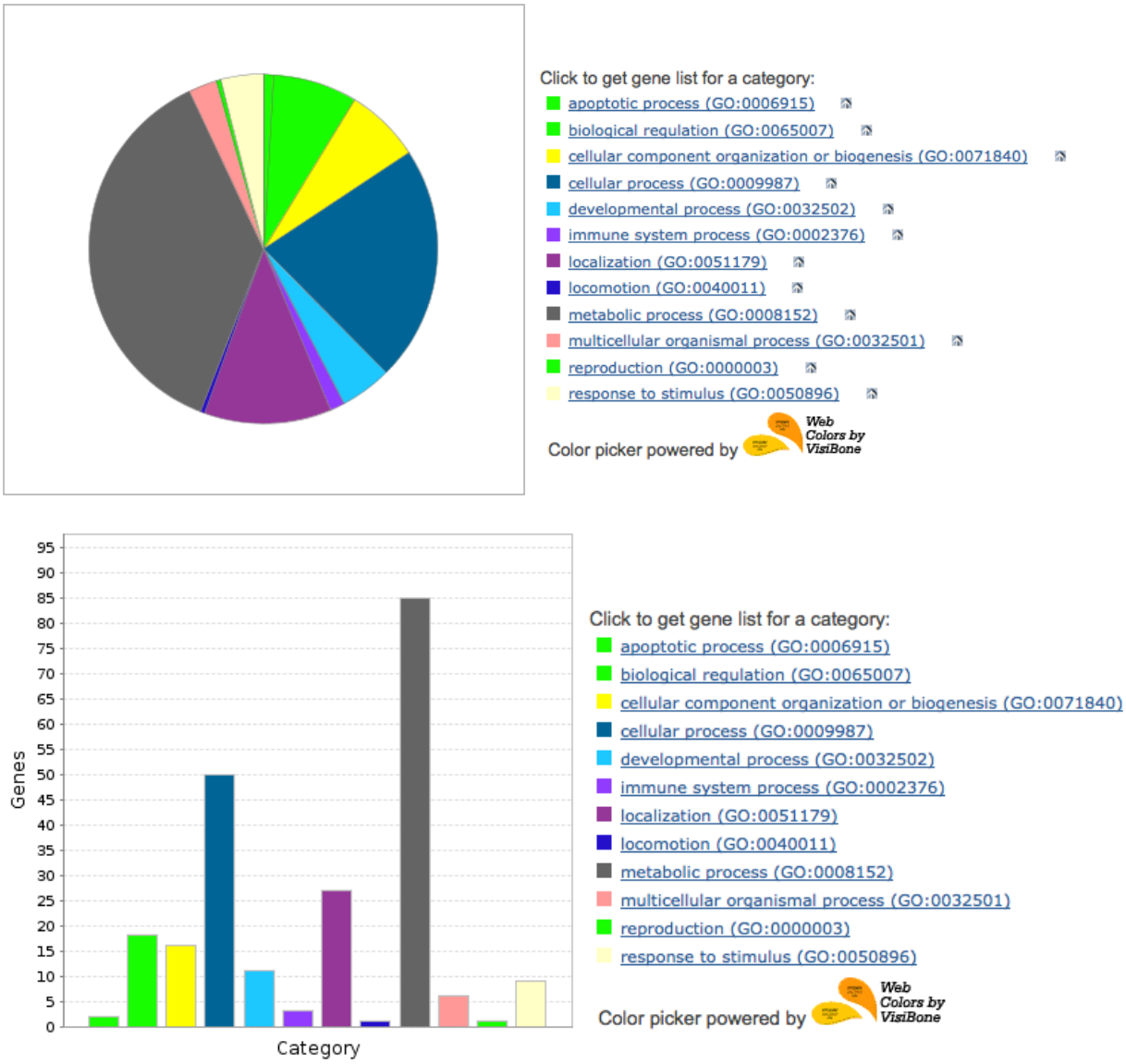

Figure S17: Analysis of the biological function of the 128 proteins identified in the p53 K-CLIP using Panther GO-Slim (pantherdb.org).[1] A) Pie chart showing the relative percentage of proteins in each biological function classification. B) Bar graph showing the number of genes represented in each biological process. The largest gene pool of 85 genes (37%) were associated with metabolic processes (brown) and included many proteins with known association with p53 (Figure 5A in manuscript and Table S1), including DNA-PK, PKR, and MRCKβ.

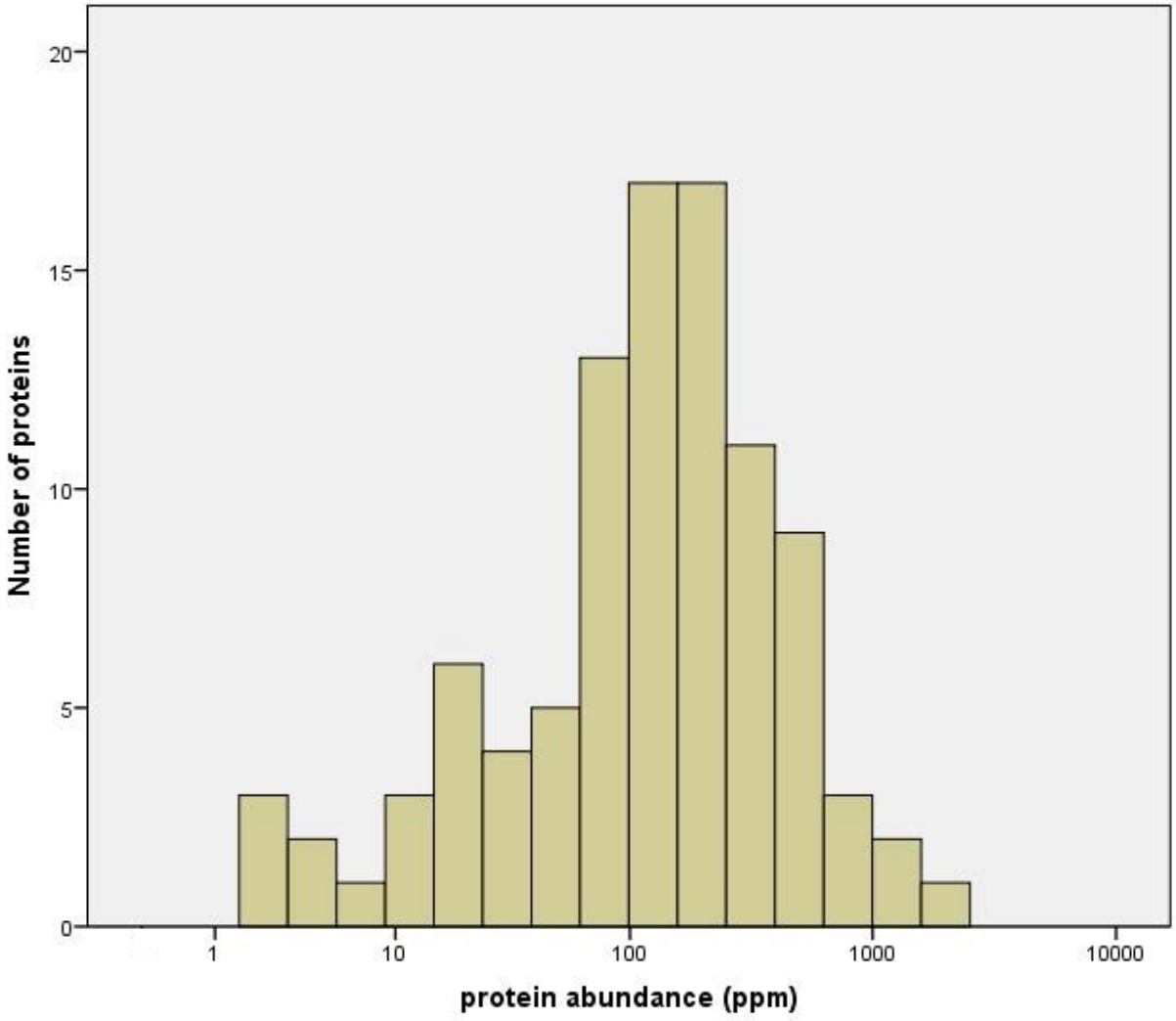

Figure S18: Abundance analysis of the proteins identified by K-CLIP. Previously published data on protein abundance in RKO cells[2] were obtained for the K-CLIP enriched proteins from Pax database[3] and then plotted. K-CLIP identified proteins with a range of abundance from 2 to 2029 ppm. The published range of protein abundance in RKO cells is from 0.01 to 10,000.

References

1. Mi, H.; Muruganujan, A.; Thomas, P. D., PANTHER in 2013: modeling the evolution of gene function, and other gene attributes, in the context of phylogenetic trees. *Nucleic Acids Res* **2013,** *41* (Database issue), D377-86.
2. Geiger, T.; Wehner, A.; Schaab, C.; Cox, J.; Mann, M., Comparative proteomic analysis of eleven common cell lines reveals ubiquitous but varying expression of most proteins. *Mol Cell Proteomics* **2012,** *11* (3), M111 014050.
3. Wang, M.; Herrmann, C. J.; Simonovic, M.; Szklarczyk, D.; von Mering, C., Version 4.0 of PaxDb: Protein abundance data, integrated across model organisms, tissues, and cell-lines. *Proteomics* **2015,** *15* (18), 3163-8.